APPLICATIONS OF
MODELLING AND SIMULATION
http://arqiipubl.com/ams eISSN 2600-8084 VOL 3, NO. 3, 2019, 125-134

CFD Simulations of Fluid Flow Characteristics in Wavy Micro-Channels with Obstructions

Ashraf Balabel[1,2*] and Abdel-Fattah Mahrous[1,2]

[1]Mechanical Engineering Department, Faculty of Engineering, Taif University, Saudi Arabia
[2]Mechanical Power Engineering Department, Faculty of Engineering, Menoufiya University, 32511, Egypt

[*]Corresponding author: ashrafbalabel@yahoo.com

Received 27 June 2019, Revised 14 July 2019, Accepted 17 July 2019.

Abstract: This work presents Computational Fluid Dynamics (CFD) simulations of laminar fluid flow characteristics through wavy micro-channels with obstructions. Two types of obstructions were computationally studied namely, cylindrically and spherically shaped obstructions. Based on the shape of obstacles, two micro-channels having the same hydraulic diameter were investigated: rectangular and cylindrical micro-channels. In addition, the position of obstructive elements next to either the crests or troughs of the wavy surface was computationally studied. The axial velocity and the corresponding pressure distributions in the transverse and longitudinal directions of flow were investigated near the regions of obstacles in order to predict the flow behavior. The computational results showed that the longitudinal and axial velocity profiles and the corresponding pressure distribution can predict the position of the obstacles through the flow stream. An important feature of the flow field can be observed in the case of spherical obstacles: the existences of negative velocity near the region of obstacles. This can be considered as a precursor of the flow separation. The region of expected flow separation would be increased by increasing the obstacle diameter as well as by increasing the flow Reynolds number. In general, the application of the present study is most appropriate to bioengineering as it resembles the study of blood flow and pressure in arteries and blood vessels where arteries are being changed in geometry and structure due to the existence of cholesterol cells.

Keywords: Computational fluid dynamics; Laminar flow; Micro-channel; Obstacles; Wavy surfaces.

1. INTRODUCTION

Recently, thermo-fluid characteristics in micro-channels have been noticed to play a significant role in many engineering as well as industrial applications. In a preliminary numerical investigation, the turbulent flow characteristics were predicted in wavy micro-channel [1]. The numerical method adopted was based on a solution of steady Reynolds-Averaged Navier-Stokes equations together with a two-layer turbulence model for a two-dimensional channel flow with a wavy wall. Although such a method has succeeded to capture the important physical features of turbulent flow in such geometry, however, unsteady simulations with suitable turbulence wall functions are required to extensively study the effect of wavy boundaries in the turbulent flow.

In a recent investigation of Assato and De Lemos [2], the performance of linear and nonlinear eddy-viscosity turbulence models was examined for predicting turbulent flow in periodically sinusoidal-wave channels. The classical wall function and a low Reynolds model were used to describe the wall flow. The obtained results showed that application of nonlinear models and the high Reynolds wall treatment were more accurate, economic and stable than linear models and the low Reynolds wall treatment. The effect of using pulsating flows inside wavy sections on heat transfer was studied using the finite volume method [3]. The obtained results showed that sinusoidal fluid pulsation can be considered as an effective method for enhancing heat transfer in wavy-channel laminar flows. The convective heat transfer enhancement in corrugated channel with wavy wall and low Reynolds number flows was studied numerically in [4]. The predicted laminar velocity field was obtained by an approximate analytical solution valid for smooth corrugations and low Reynolds numbers flow. A hybrid numerical analytical solution methodology for the energy equation based on the Generalized Integral Transform Technique was proposed.

In three-dimensional wavy micro-channels with rectangular cross section, laminar liquid–water flows with heat transfer were numerically investigated by Sui *et al.* [5]. In such a study, steady Navier–Stokes equation was solved using the Computational Fluid Dynamics (CFD) software package, FLUENT. The obtained results showed that the quantity and the location of the vortices may change along the flow direction. This can greatly enhance the convective fluid mixing and the heat transfer performance as compared to straight micro-channels with the same cross section. The thermal and hydrodynamic characters of a hydrodynamically and thermally developing flow in a wavy micro-channel were numerically analysed by Shokouhmand and Bigham [6]. The effect of creep flow on thermal and hydrodynamic characters of flow in wavy micro-channels was investigated. It was found that the amplitude of the wave has a large effect on the variation of the flow characteristics in the wavy region.

In further three-dimensional numerical investigation of laminar fluid flow and heat transfer, the effect of the wavy feature amplitude, wavelength, and aspect ratio for different Reynolds numbers between 50 and 150 on improving the heat transfer performance was investigated by Gong *et al*. [7]. It was concluded that, the performance of wavy channels exceeded the performance of a straight channel for Reynolds number, *Re* = 50 by up to 55% for the best aspect ratio considered. In order to understand the fundamentals of fluid flow in the wavy micro-channels for different Reynolds number, flow measurements were made by Gong *et al*. [8] using micro-Particle Image Velocimetry (PIV) technique in addition to three-dimensional laminar fluid flow and heat transfer numerical simulation. It was found that, wavy channels provided an improvement of up to 26% in the overall performance in comparison with micro-channels with straight walls applied for cooling electronics. Recently, numerical simulation of fluid mixing in a floor-grooved micro-channel with wavy sidewalls was numerically investigated by Lin *et al*. [9]. The obtained results showed that the effects of the wavy sidewalls of the present micromixer on the enhancement of fluid mixing increase with the increase of Reynolds number. Moreover, the degree of mixing increases with increasing of the corrugation angle.

More recently, the hydrodynamic and thermal behaviors of turbulent flow in wavy micro-channel were numerically investigated using a new numerical method based on control volume approach that so-called fraction-step method along with the standard k-epsilon turbulence model [10]. The effects of Reynolds number on the flow characteristics were extensively investigated. An extensive investigation of low Reynolds number turbulent flow in a narrow and wavy channel was performed by Al-Muhammad *et al*. [11]. Different low Reynolds number turbulence models have been applied for such flow and configurations. Remarkable differences were observed between the different low Reynolds number models. It was concluded that the classical turbulent models cannot reproduce the characteristics of such a flow. It was recommended that further three-dimensional simulations are required to determine the best turbulence model for describing such a flow.

Introducing a number of obstacles in the micro-channels is a novel method for mixing in micro-fluidic devices and provides useful information applied for the design of these devices. The previous results indicated that asymmetric placement of the obstacles has more effect on the mixing than the number of obstacles [12]. Moreover, simple cylindrical obstacles (i.e. pillars) in the micro-channel, tends to create a lateral net secondary flow inside the channel which resembles the recirculating mean flow. This passive method produces the possibility of exceptional control of the 3D structure of the fluid within micro-fluidic devices. More recently, experimental measurements for hydrodynamics and heat transfer characteristics downstream of channel obstruction in micro-fluidic systems were performed in laminar flow regime [13]. The flow field was measured using PIV while the heat transfer characteristics were measured using infrared (IR) thermography of a Joule-heated foil.

It should be pointed out that, the numerical simulation of flow inside wavy micro-channel has received a great attention in different engineering sciences such as two-phase flow and nanofluids with the aim of enhancement of heat transfer characteristics [14 - 18]. Consequently, the main objective of the present work was to computationally study the laminar fluid flow in wavy micro-channels with obstructions. Two types of obstructions, differ in shape, were computationally investigated; cylindrical and spherical. The configuration of wavy micro-channel section was chosen to match with the appropriate shape of obstacles. The 3D computational simulations were performed by using ANSYS Fluent 15.

2. GOVERNING EQUATIONS AND COMPUTATIONAL METHOD

Hydrodynamics of fluid flow in a wavy micro-channel were computationally calculated using a finite volume commercial CFD solver, ANSYS Fluent 15. The governing equations of the fluid (water) flow throughout the wavy micro-channel are the mass and momentum conservation equations. The flow regime considered in the present study was laminar and the problem was three dimensional. The governing equations of mass and momentum are written in steady state condition as [19]:

$$\frac{\partial}{\partial x_j}\left(\rho u_j\right) = 0 \tag{1}$$

$$u_j \frac{\partial}{\partial x_j}\left(\rho u_i\right) = -\frac{\partial P}{\partial x_i} + \frac{\partial}{\partial x_j}\left[\mu\left(\frac{\partial u_i}{\partial x_j}\right)\right] \tag{2}$$

SolidWorks CAD software was used for building and exporting the 3D geometry of the wavy micro-channel test models. The model geometry with configuration shown in Figure 1 consists of three sections: an inlet section with straight walls, a wavy surface section of 16 mm length, and an exit section with straight walls. The entrance section with straight walls has been assigned an enough length in the flow direction to ensure a fully developed flow at the inlet of the wavy section. The micro-channel aspect ratio is 1. A uniform inlet fluid velocity profile was specified at the inlet boundary of the test section, while a pressure outlet boundary condition was assigned at the outlet section.
The equation of wavy surface is given as:

$$y = A\sin\left(\frac{2\pi}{\lambda}x\right) \tag{3}$$

where y is the vertical coordinate, x is the longitudinal coordinate, A is the wave amplitude and λ is the wavelength.

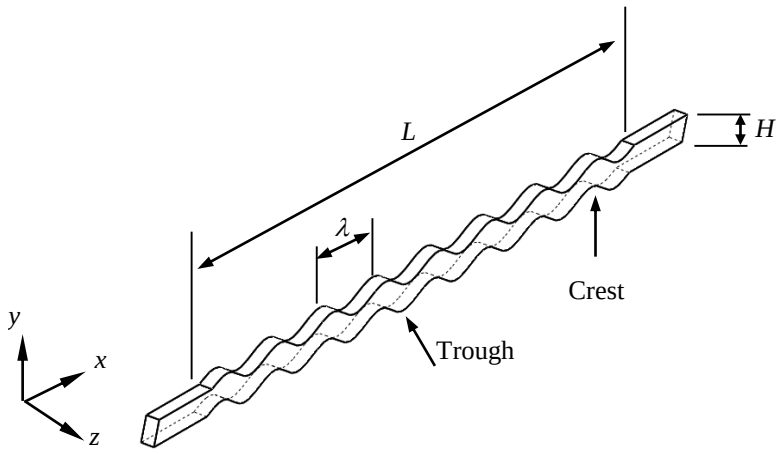

Figure 1. Configuration of wavy micro-channel model. Half of the domain was computationally modelled

To have a better relation between pressure and velocity, the Semi-Implicit Method for Pressure-Linked Equation-Consistent (SIMPLEC) algorithm was chosen during the simulations. The SIMPLEC algorithm uses a relationship between velocity and pressure corrections to enforce mass conservation and to obtain the pressure field [19]. Second order upwind discretization in momentum was applied throughout the calculations. Besides, no-slip conditions for the velocity components and zero normal pressure gradients were set as the boundary conditions for solid walls. A solution convergence tolerance of 10^{-6} was assigned to the simulations.

3. RESULTS AND DISCUSSION

3.1 CFD Model Verification and Validation

To ensure grid-solution independency as well as improved accuracy of computational results, a grid independence study has been performed for different configurations (i.e. configurations with and without obstacles). The analysis compared the computational results of three grid resolutions for each model configuration. The number of cells for the cylindrical obstacles case, for example, were 252643 (Grid I), 430716 (Grid II, reference case) and 683475 (Grid III) with mesh densities of 100888, 171998 and 272932 cells/mm^3, respectively. As shown in Figure 2(a), there is a good agreement between the results of mesh resolutions of Grid II and Grid III in terms of laminar flow axial velocity across the wavy micro-channel. The CFD results were obtained at a section away from the inlet one. Therefore, the mesh resolution for Grid II (Reference Case) is considered to give grid-independence results. Figure 2(b) shows the computational grid for Grid II of cylindrical obstacles.

Additionally, to verify the validity of the present CFD model, the obtained predicted results of the micro-channel case without obstacles were compared with results predicted by Gong *et al*. [7] under the same working conditions. Comparisons implied comparing the predicted results for straight channels as well as for wavy channels of the present and Gong *et al*. [7] models. Figure 3 compares the predicted results for pressure difference between inlet and outlet of the channel for both the present model and the model of Gong *et al*. [7]. Test runs were conducted at low Reynolds number of 50, 100 and 150. Three wave amplitudes of 0 (straight channel), 150 and 200 μm were compared. It is clear that the present CFD results match very well with results predicted by Gong *et al*. [7].

Comparisons of predicted spatial velocity profiles across the channel for both the present model and the model of Gong et al. [7] are presented in Figure 4 at Reynolds number of 100. Velocity profiles of *x*-velocity component were drawn between crests (Figure 4(a)) and troughs (Figure 4(b)) at wave amplitude of 200 μm and a wavelength of 2.0 mm. As can be seen, results predicted by the present model are very similar to predictions by Gong *et al*. [7]. As illustrated so far, the comparison between the predicted CFD results of the present model and the data predicted by Gong *et al*. [7] demonstrates a good degree of agreement. Accordingly, the present CFD model may be used to predict the flow behavior in a wavy micro-channel under different parametric predictive studies.

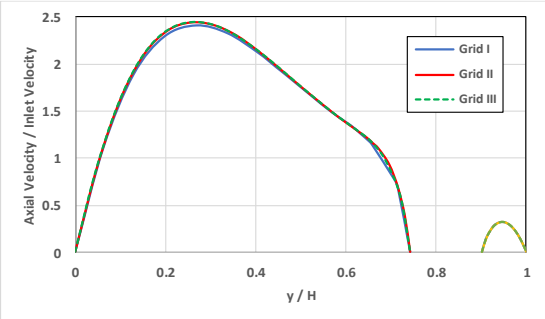

Figure 2(a). Grid independence study results

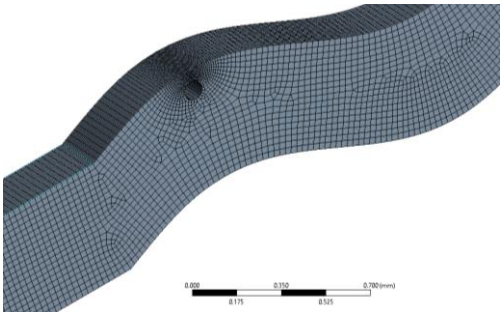

Figure 2(b). Computational grid configuration for Grid II for a wavy micro-channel with obstacles close to crest

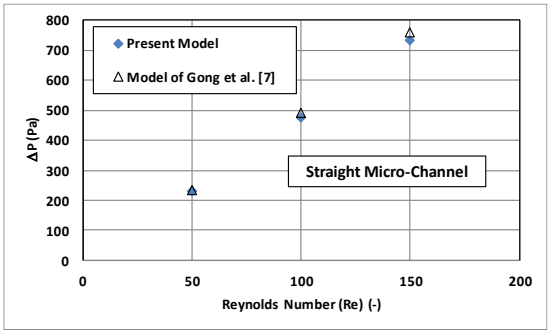

(a)

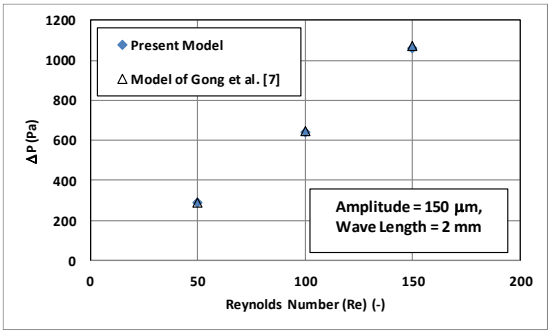

(b)

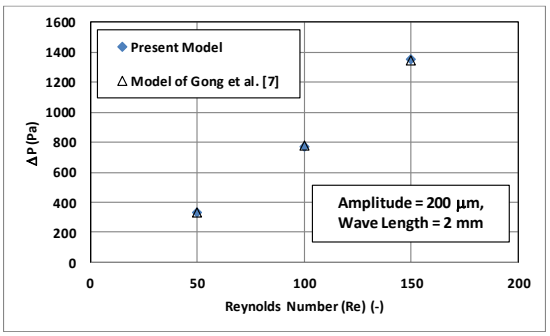

(c)

Figure 3. Comparison of predicted pressure difference across the micro-channel for both the present model and the model of Gong *et al.* [7]

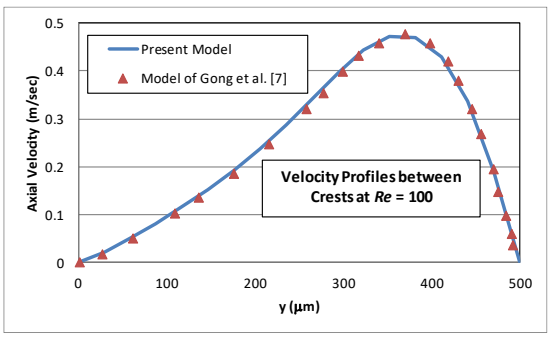

(a)

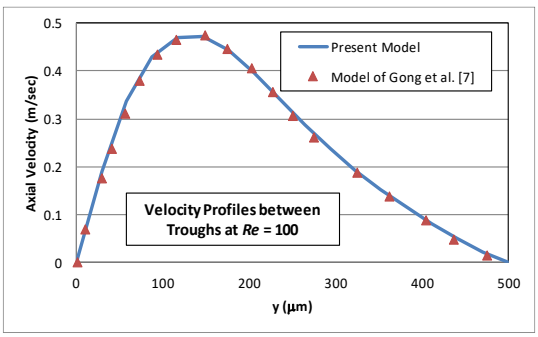

(b)

Figure 4. Comparison of predicted spatial velocity profiles across the channel for both the present model and the model of Gong *et al.* [7] at the midsection of the micro-channel for wave amplitude and length respectively of 200 µm and 2.0 mm. Type of channels are serpentine channels

3.2 Rectangular Wavy Micro-channel with Cylindrical Obstacles

Figure 5 shows different cases of the rectangular wavy micro-channel with cylindrical obstacles (80 µm diameter) placed in different positions inside the micro-channel and through the flow stream. The hydraulic diameter of the wavy micro-channel is 500 µm. The obstacles were located close to the compression side of either the upper or lower wavy surface, where the flow velocity is low. The centers of obstacles are located 90 µm away from the wavy channel walls. The reference case is case I, where there are no obstacles placed inside the micro-channel.

The effects of placing the obstacles are clearly visible in Figures 6(a) and 6(b) for the transverse axial velocity profile at the location of the obstacles. The transverse axial velocity approaches zero as the flow hits the obstacle. A second velocity distribution is developed behind the obstacles in front of the next upper/lower wall. When comparing with the reference case (Case I, without obstacles), it can be noticed that there is an increase in the maximum value of the transverse velocity due to the second velocity distribution, although the trend of the velocity profile is the same in both cases with a slightly difference when the flow approaches the obstacle. The pressure distribution shown in the lower graphs of Figures 6(a) and 6(b) reveal the position of the obstacles in the flow stream by a slightly decrease before approaching the obstacles and a slightly increase after the obstacles and next to the channel wall. Apart from the obstacles, an increase in the transverse axial velocity is noticed throughout the channel section as illustrated in the upper graphs of Figures 6(a) and 6(b). Both the velocity and the pressure profiles in the transverse direction can be used for the detection of the obstacles position in a normal way. Although the transverse axial velocity profiles seem to be a mirror of each other in both cases where obstacles are closer to crests and troughs, the magnitude of the corresponding pressures are different despite similarity in behavior.

Figures 7(a) and 7(b) show the longitudinal axial velocity and pressure distributions across the centerline of cylindrical obstacles of 80 µm diameter closer to upper and lower crests, respectively. The effect of obstacles can be seen from the velocity profile by approaching zero velocity at the boundary of the obstacles and the pressure distribution is similar to that obtained from the classical flow over circular cylinder, i.e. the obstacle front point that faces the oncoming fluid flow experiences the highest pressure while the back point is subjected to the lowest pressure. Also, as mentioned before, the longitudinal axial velocity profiles and the corresponding pressure distribution can predict the position of the obstacles through the flow stream. Figures 8(a) and 8(b) show the effect of Reynolds number on the transverse velocity profiles and the transverse pressure distribution in Case II and Case III. For both cases, the figures show that a normal behavior of velocity and pressure profiles, where the increase in Reynolds number leads to an increase in velocity as well as pressure values. These results were obtained either in front or back of the obstacles.

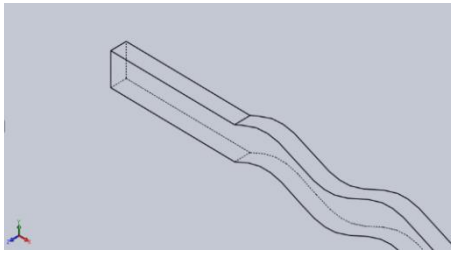

Case I: Rectangular wavy micro-channel without obstacles

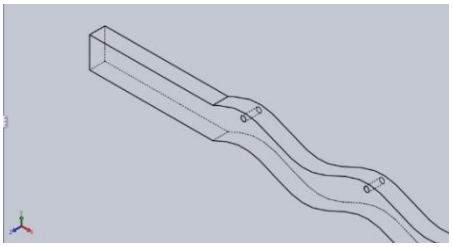

Case II: With cylindrical obstacles closer to upper crests

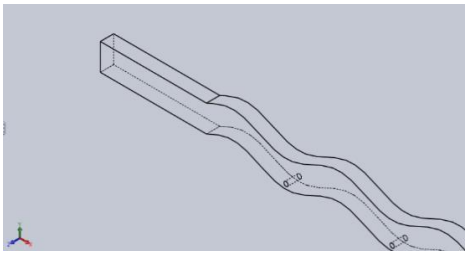

Case III: With cylindrical obstacles closer to lower troughs

Figure 5. Rectangular wavy micro-channel with cylindrical obstacles test cases

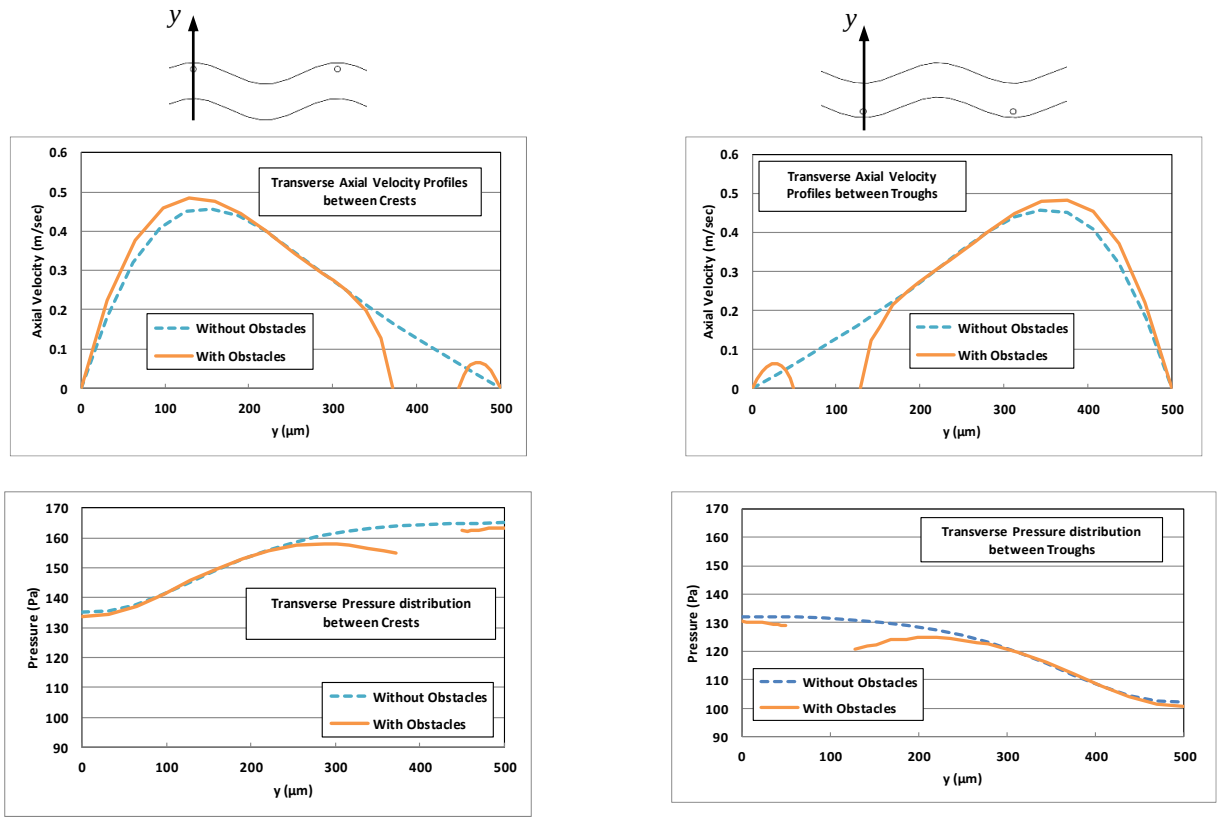

(a) Obstacles closer to upper crests (b) Obstacles closer to lower troughs

Figure 6. Transverse axial velocity and pressure distributions across the centerline of cylindrical obstacles of 80 μm diameter: (a) Obstacles closer to upper crests, (b) Obstacles closer to lower troughs. *Re*=100, Amplitude = 150 μm, λ=2.0 mm

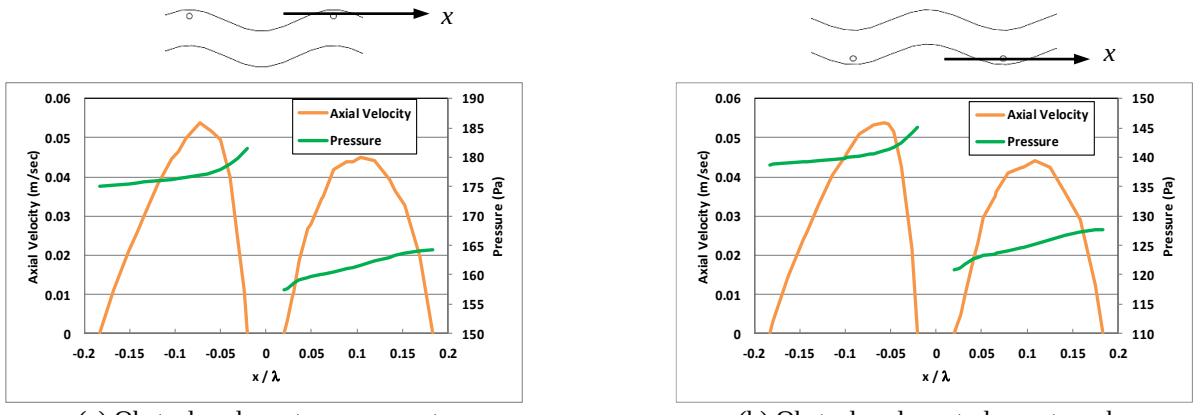

(a) Obstacles closer to upper crests (b) Obstacles closer to lower troughs

Figure 7. Longitudinal axial velocity and pressure distributions across the centerline of cylindrical obstacles of 80 μm diameter: (a) Obstacles closer to upper crests, (b) Obstacles closer to lower troughs. *Re*=100, Amplitude = 150 μm, λ=2.0 mm

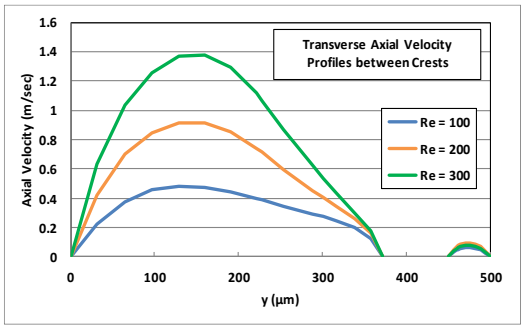

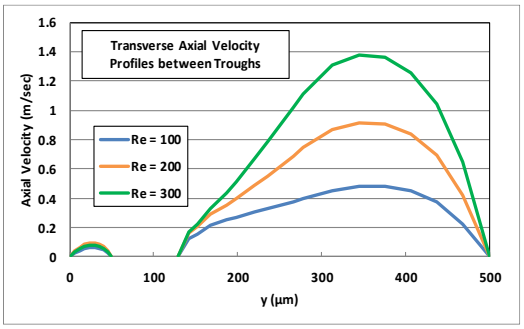

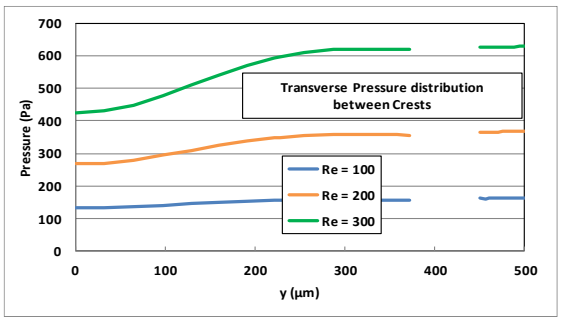

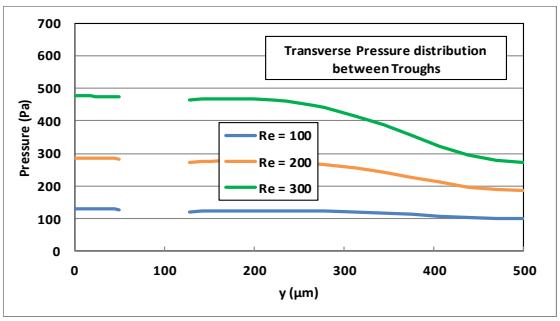

(a) Obstacles closer to upper crests (b) Obstacles closer to lower troughs

Figure 8. Effects of *Re* on transverse axial velocity and pressure distributions across the centerline of cylindrical obstacles of 80 μm diameter: (a) Obstacles closer to upper crests, (b) Obstacles closer to lower troughs. Amplitude = 150 μm, λ=2.0 mm

3.3 Cylindrical Wavy Micro-channel with Spherical Obstacles

In this section, a cylindrical wavy micro-channel, having the same hydraulic diameter as the rectangular one (500 μm), is considered in order to show the effect of geometric shape of the wavy channel on the flow behavior. Moreover, the obstacles were considered to be with a spherical shape having a diameter of 80 μm and located on the same positions as mentioned before in rectangular micro-channel case. Figure 9 shows the configuration of the cylindrical wavy micro-channel with and without spherical obstacles.

Figure 10(a), presents the axial velocity distribution in the transverse direction for the cases with and without obstacles. The obstacles were placed closer to the upper crest. The velocity profile in the wavy micro-channel with obstacles shows smaller amplitude velocity profile in comparison with the case without obstacles. In contrast to the rectangular geometry, Figures 6(a) and 6(b), the velocity profile in case of obstacles did show no peak behind the obstacles, only a similar distribution to that of cylindrical wavy channel without obstacles. This can be referred to the nature of the flow field in 3D cylindrical coordinates. This remark can also be approved from the pressure distribution, where only an increase in the pressure values due to the placement of the obstacles in the flow field without any remarkable variation along the transverse direction. Furthermore, reverse flow (or flow separation) is clearly noticed near the location of obstacles. Figure 10(b) shows the axial velocity distribution and the pressure value in the transverse direction at the center of the minimum area of the wavy micro-channel. In comparison, with the case of no obstacles, the velocity as well as the pressure profiles showed an increase in the velocity and pressure values due to obstacles. Moreover, a similar profile in front and back of the obstacles have been obtained. The pressure profile is similar to the classical profile of pressure distribution over a sphere, indicating the effect of placing the obstacles in through the flow field at the smaller cross section of the channel. Figure 11 shows the variation of the longitudinal axial velocity and pressure across the centerline of the obstacles located at the narrow area of the channel. An important feature of the flow field can be observed namely, the existing of negative velocity directly downward the obstacles. This can be considered as a precursor of the flow separation. A nearly constant pressure profiles can also be observed downward the obstacles due to the existing of separation zone. Figure 12 demonstrates two counter rotating vortices behind the spherical obstacles.

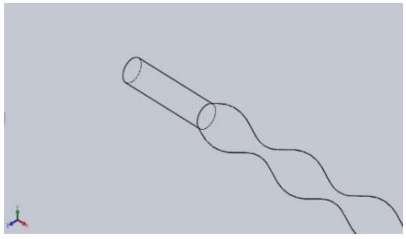

Case I: Cylindrical Wavy micro-channel without obstacles

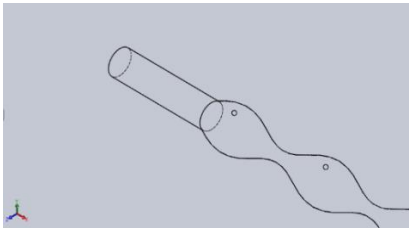

Case II: With spherical obstacles closer to upper crests

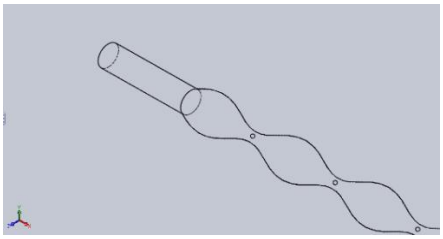

Case III: With spherical obstacles at the center of narrow section

Figure 9. Cylindrical wavy micro-channel with spherical obstacles test cases

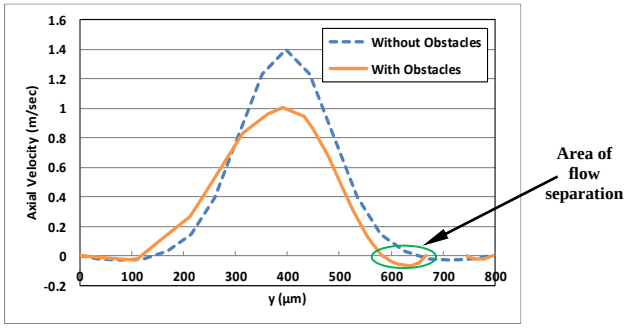

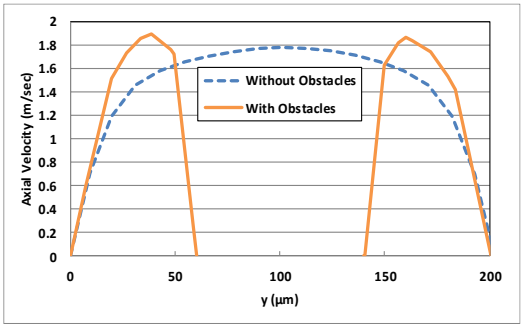

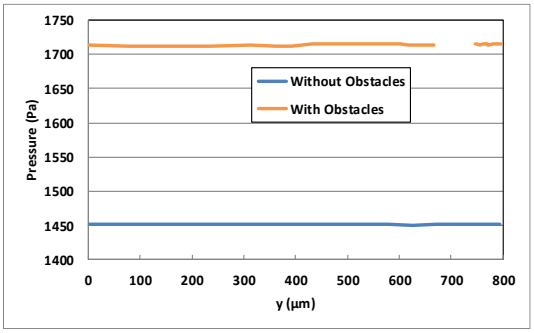

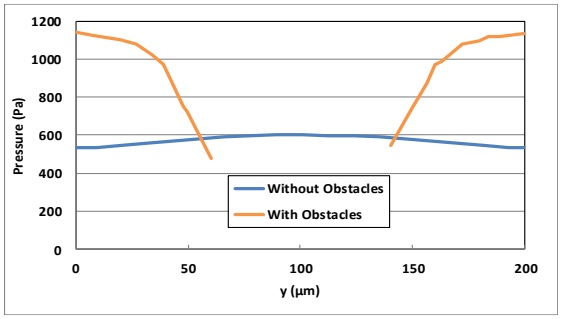

(a) Obstacles closer to upper crests

(b) Obstacles at the channel center of minimum area

Figure 10. Transverse axial velocity and pressure distributions across the centerline of spherical obstacles of 80 µm diameter: (a) Obstacles closer to upper crests, (b) Obstacles at the center of minimum flow area. *Re*=100, Amplitude = 150 µm, λ=2.0 mm

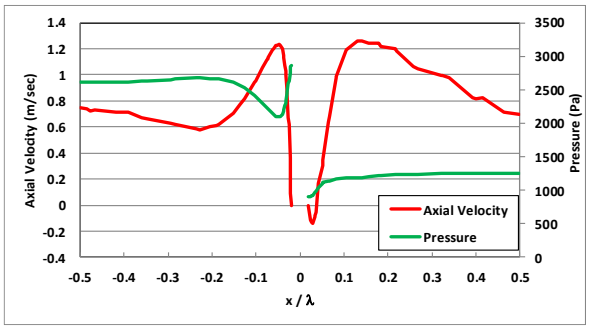

Figure 11. Longitudinal axial velocity and pressure distributions across the centerline of spherical obstacles of 80 µm diameter located at the center of minimum flow area. *Re*=100, Amplitude = 150 µm, λ=2.0 mm

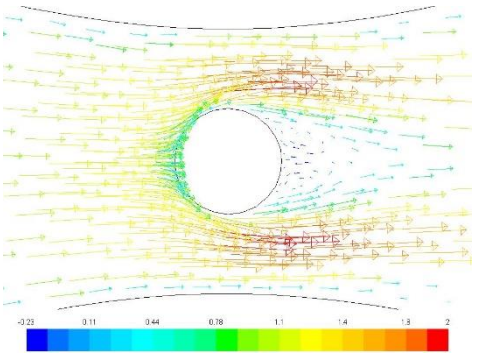

Figure 12. Velocity vectors (in m/sec) at the symmetry plane of cylindrical wavy micro-channel. Spherical obstacles of 80 µm diameter are located at the center of minimum flow area. *Re*=100, Amplitude = 150 µm, λ=2.0 mm

Figure 13 shows the effect of obstacle diameter on transverse (a) and longitudinal (b) axial velocity and pressure distributions across the centerline of spherical obstacles located at the center of minimum area of the channel. Three diameters have been considered; 60 µm, 80 µm and 100 µm. In case of predicting the axial velocity in the transverse direction, there is an increase of the velocity amplitude in front and backward the obstacles by increasing the obstacle diameter. By predicting the longitudinal axial velocity, it is observed that the extent of the separation can be much lesser by decreasing the obstacle

diameter. The pressure profiles in the transverse and longitudinal directions show a normal behavior, where there is an increase of the pressure values by increasing the obstacle diameter.

Figure 14 shows the effect of Reynolds number on the transverse axial velocity distributions as well as the pressure profiles in case of placing the obstacles either closer to upper crest or in the narrow area of the channel. A normal behavior of the velocity distribution as well as the pressure values have been obtained in such a manner that by increasing the Reynolds number the values are increased. An important feature can be observed for the transverse axial velocity is the appearance of a separation zone in front of the obstacles with an extent increase by increasing the Reynolds number.

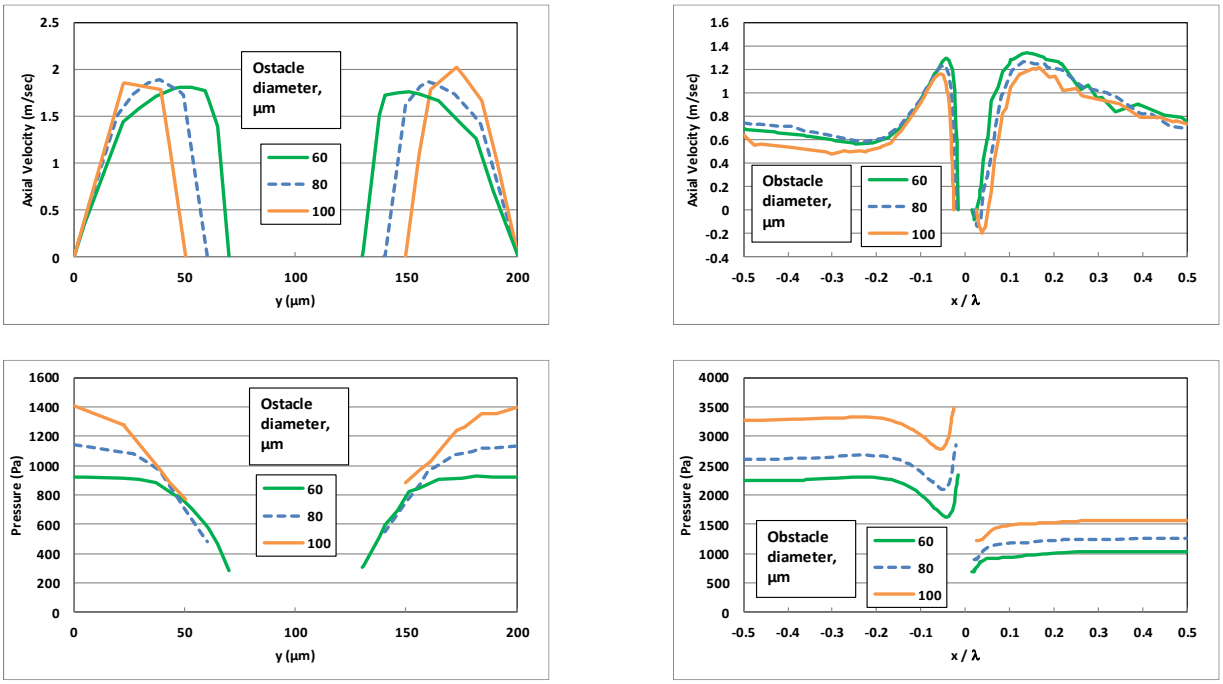

(a) Transverse distributions of axial velocity and pressure (b) Longitudinal distributions of axial velocity and pressure

Figure 13. Effect of obstacle diameter on transverse (a) and longitudinal (b) axial velocity and pressure distributions across the centerline of spherical obstacles of 80 μm diameter located at the center of minimum flow area. *Re*=100, Amplitude = 150 μm, λ=2.0 mm

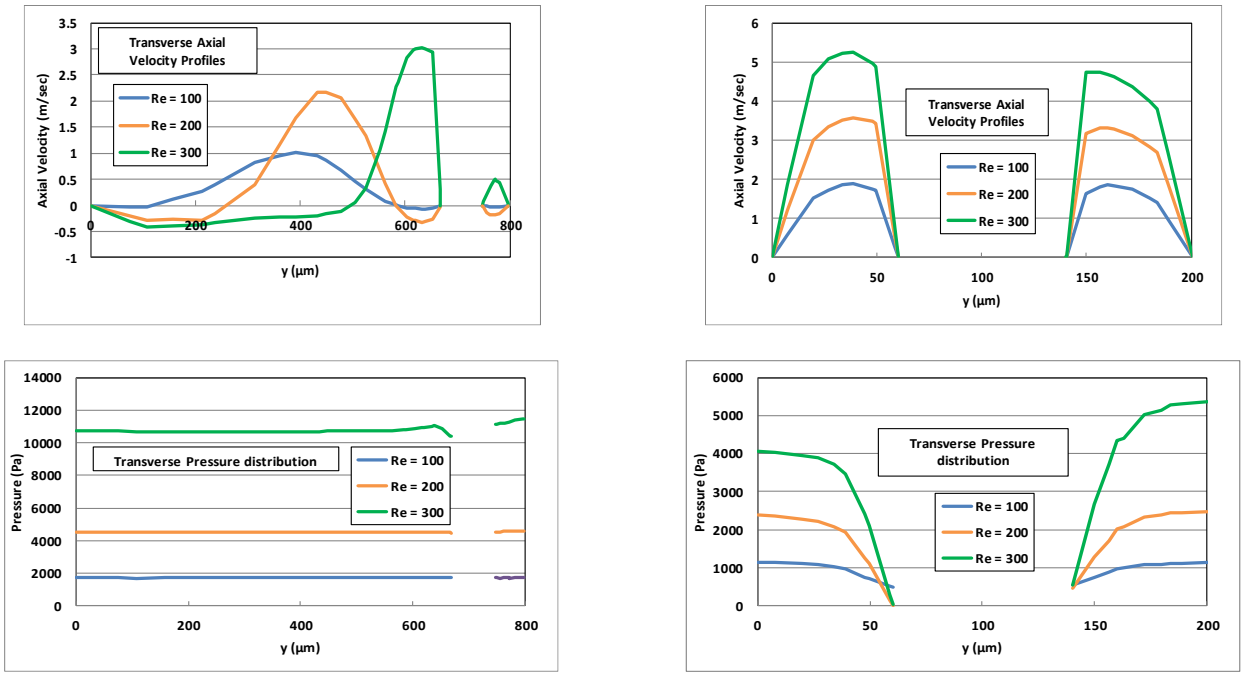

(a) Obstacles closer to upper crests (b) Obstacles at the channel center of minimum area

Figure 14. Effects of *Re* on transverse axial velocity and pressure distributions across the centerline of spherical obstacles of 80 μm diameter: (a) closer to upper crests, (b) at channel center of narrow section. Amplitude = 150 μm, λ=2.0 mm

4. CONCLUSION

The present work aims to computationally study (using CFD) laminar fluid flow characteristics through a wavy micro-channel with flow obstructions. Two types of obstacles were computationally studied, namely cylindrically and spherically shaped obstacles. Fluid field characteristics in two micro-channel sections having the same hydraulic diameter and associated with the appropriate shape of obstacles were computational investigated, namely rectangular and cylindrical micro-channels. The axial velocity and the corresponding pressure profiles in both the transverse and longitudinal directions of flow were investigated near the regions of obstacles in order to understand the flow behavior. Owing to the obstacles, the CFD results showed that an increase in both the axial velocity and pressure is noticed throughout the micro-channel section. An important flow characteristic regarding the flow separation was observed next to the obstacles. By increasing the obstacles diameter or flow Reynolds number, the extent of separation zone would also increase. The presented results of axial velocity and pressure distributions around the obstacles can predict, in accurate manner, the position of the obstacles in flow despite its small diameter. The obtained CFD results are encouraging to extend the presented computational model to predict the bio-fluid dynamics, especially the blood flow and pressure in the interior system of arteries or when arteries are being changed in geometry and structure due to the existence of cholesterol cells. Moreover, the present computational model can be also used in the healthcare field, where microfluidic devices containing microchannels have shown an increasing number of applications in the biological and clinical areas.

REFERENCES

[1] V. Patel, J. T. Chon and J. Yoon, Turbulent flow in a channel with a wavy wall, *Journal of Fluids Engineering*, 113(4), 579-586, 1991.

[2] M. Assato and M. J. De Lemos, Turbulent flow in wavy channels simulated with nonlinear models and a new implicit formulation, *Numerical Heat Transfer, Part A: Applications*, 56(4), 301-324, 2009.

[3] E. M. Alawadhi and R. I. Bourisli, The role of periodic vortex shedding in heat transfer enhancement for transient pulsatile flow inside wavy channels, *International Journal of Natural Sciences and Engineering*, 1(2), 79-85, 2009.

[4] F. V. Castellões, J. N. Quaresma and R. M. Cotta, Convective heat transfer enhancement in low Reynolds number flows with wavy walls, *International Journal of Heat and Mass Transfer*, 53(9), 2022-2034, 2010.

[5] Y. Sui, C. J. Teo, P. S. Lee, Y. T. Chew, and C. Shy, Fluid flow and heat transfer in wavy microchannels, *International Journal of Heat and Mass Transfer*, 53(13-14), 2760-2772, 2010.

[6] H. Shokouhmand and S. Bigham, Effects of entrance region transport processes on slip flow regime in a wavy wall microchannel with isothermally heated walls, *Proceedings of the World Congress on Engineering*, London, 2010, pp. 1-6.

[7] L. J. Gong, K. Kota, W. Tao and Y. Joshi, Parametric numerical study of flow and heat transfer in microchannels with wavy walls, *Journal of Heat Transfer*, 133(5), 051702, 2011.

[8] L. J. Gong, K. Kota, W. Tao and Y. Joshi, Thermal performance of microchannels with wavy walls for electronics cooling, *IEEE Transactions on Components, Packaging and Manufacturing Technology*, 1(7), 1029-1035, 2011.

[9] Y. –S. Lin, C. –Y. Wu and Y. –C. Chu, Numerical study of fluid mixing in a grooved micro-channel with wavy sidewalls, *International Journal of Mechanical and Mechatronics Engineering*, 7(7), 1419-1423, 2013.

[10] A. Balabel and A. Khadrawi, Numerical simulation of turbulent thermo-fluid dynamics in wavy microchannel, *International Journal of Energy Science and Engineering*, 1(3), 100-105, 2015.

[11] J. Al-Muhammad, S. Tomas and F. Anselmet, Modeling a weak turbulent flow in a narrow and wavy channel: case of micro-irrigation, *Irrigation science*, 34(5), 361-377, 2016.

[12] H. Wang, P. Iovenitti, E. Harvey and S. Masood, Optimizing layout of obstacles for enhanced mixing in microchannels, *Smart Materials and Structures*, 11(5), 662-667, 2002.

[13] A. Waddell, J. Punch, J. Stafford and N. Jeffers, The hydrodynamic and heat transfer behavior downstream of a channel obstruction in the laminar flow regime, *International Journal of Heat and Mass Transfer*, 101, 1042-1052, 2016.

[14] A. Sakanova, J. Zhao and K. –J. Tseng, Investigation on the influence of nanofluids in wavy microchannel heat sink, *IEEE Transactions on Components, Packaging and Manufacturing Technology*, 5(7), 956-970, 2015.

[15] N. Tiwari and M. K. Moharana, Two-phase flow conjugate heat transfer in wavy microchannel, *Proceedings of ASME 16th International Conference on Nanochannels, Microchannels, and Minichannels,* Croatia, 2018, pp. 1-8.

[16] L. Lin, J. Zhao, G. Lu, X. –D. Wang and W. –M. Yan, Heat transfer enhancement in microchannel heat sink by wavy channel with changing wavelength/amplitude, *International Journal of Thermal Sciences*, 118, 423-434, 2017.

[17] Z. Parlak, Optimal design of wavy microchannel and comparison of heat transfer characteristics with zigzag and straight geometries, *Heat and Mass Transfer*, 54(11), 3317-3328, 2018.

[18] P. K. Singh, D. S. Naruka and P. S. Lee, Numerical investigation of flow and heat transfer of nanofluids in a wavy microchannel, *International Journal of Energy for a Clean Environment*, 19(1), 19-35, 2018.

[19] ANSYS Fluent, Fluent 15.0 User's Guide, Fluent Incorporated, Lebanon, NH, 2015.